



High frequency of new particle formation events driven by summer monsoon in the central Tibetan Plateau, China

Lizi Tang¹, Min Hu^{*1,2}, Dongjie Shang¹, Xin Fang¹, Jianjiong Mao², Wanyun Xu³, Jiacheng Zhou⁴, Weixiong Zhao⁴, Yaru Wang¹, Chong Zhang¹, Yingjie Zhang⁵, Jianlin Hu², Limin Zeng^{1,2}, Chunxiang Ye¹, Song Guo^{1,2}, Zhijun Wu^{1,2}

5 ¹State Key Joint Laboratory of Environmental Simulation and Pollution Control, International Joint Laboratory for Regional Pollution Control, Ministry of Education (IJRC), College of Environmental Sciences and Engineering, Peking University, Beijing 100871, China

²Collaborative Innovation Center of Atmospheric Environment and Equipment Technology, Jiangsu Key Laboratory of Atmospheric Environment Monitoring and Pollution Control. Nanjing University of Information Science & Technology,
10 Nanjing 210044, China

³State Key Laboratory of Severe Weather & Key Laboratory for Atmospheric Chemistry of CMA, Institute of Atmospheric Composition, Chinese Academy of Meteorological Sciences, Beijing, 100081, China

⁴Laboratory of Atmospheric Physico-Chemistry, Anhui Institute of Optics and Fine Mechanisms, HFIPS, Chinese Academy of Science, Hefei 230031, Anhui, China

15 ⁵School of Ecology and Nature Conservation, Beijing Forestry University, Beijing 100083, China

Correspondence to: Min Hu (minhu@pku.edu.cn).

Abstract

New particle formation (NPF) is an important source of cloud condensation nuclei (CCN), which affects Earth's
20 radiative balance and global climate. The mechanism and CCN contribution of NPF at the high-altitude mountains, especially in the Tibetan Plateau (TP), was unclear due to lack of measurements. In this study, intensive measurements were conducted at Nam Co station (4379 m a.s.l.) in the central TP during both pre-monsoon and summer monsoon seasons. The frequencies of NPF events exhibited extreme distinction with 15% in pre-monsoon season and 80% in monsoon season. The level of organic vapours governed the occurrence of NPF events, while condensation sink and gaseous sulfuric acid had no
25 effect. The frequent NPF events in summer monsoon season resulted from the higher concentration of organic vapours, which was brought from northeast India by the strong southerly monsoon. It had increased the aerosol number concentrations and CCN at supersaturation of 1.2% by more than 2 and 0.5 times compared with those in pre-monsoon season, respectively. Considering that the smaller particles formed by NPF may further grow and reach CCN size during the



following days due to the low-level coagulation sink, the amount of potential CCN in monsoon season could be much larger
30 than our local measurement results. Our results emphasized the importance of organics to NPF in high-altitude atmosphere,
and the seasonal effect of NPF at the high-altitude sites should be carefully considered in model simulations to reduce the
uncertainty of global CCN budget.

1 Introduction

Atmospheric aerosols can affect Earth's radiative balance through direct interaction with solar radiation and by serving
35 as cloud condensation nuclei (CCN), and thus global climate. There is considerable uncertainty about the total radiative
forcing contributed by aerosol particles, mainly from the number concentrations and sizes of CCN (IPCC, 2021). New
particle formation (NPF) is a physical and chemical process, comprising nucleation of gaseous precursors and the
subsequent growth of the nucleated clusters into aerosol particles. NPF has been considered to be an important source of
aerosols and contribute a major fraction to the global CCN budget. Model simulations found that up to 45% of global CCN
40 were secondary aerosols derived from NPF process, with a large fraction created in the free troposphere (Merikanto et al.,
2009). Furthermore, NPF may be more important to the total CCN budget in the pristine atmosphere than that in the
industrial atmosphere (Gordon et al., 2017).

With the development of technology and instrumentation, NPF events have been observed in diverse atmospheric
environments around the world, including urban, rural, mountain, boreal, and polar regions (Nieminen et al., 2018;
45 Kerminen et al., 2018; Wang et al., 2017; Peng et al., 2014). High-altitude mountains are particularly interesting
environment for atmospheric NPF studies due to near absence of primary particle sources and long aerosol particle lifetimes
in such environment (Kerminen et al., 2018). Furthermore, the NPF events at the high-altitude sites have been considered as
a potentially important source of particles injected into the free troposphere (Venzac et al., 2008). Unfortunately, there were
few NPF studies at pristine high-altitude sites, mainly due to the challenges in measuring particle numbers and precursors
50 under the adverse meteorological and topographic conditions such as the extremely low temperature, the thin air and the
steep mountains. Moreover, the parameters and the exact mechanisms of NPF in the limited high-altitude measurements
showed large temporal and spatial variations. For example, variable frequencies of NPF event days were found: 20% during
one year at Jungfrauoch, Switzerland (3580 m a.s.l) (Tröstl et al., 2016a), 56% in spring and 43% in summer at Storm Peak
Laboratory, USA (3210 m a.s.l) (Haller et al., 2011), 67% during one year in Maïdo observatory, Réunion (2165 m a.s.l)
55 (Rose et al., 2019), and 80% in post-monsoon season at Mt. Daban, China (3295 m a.s.l) (Du et al., 2015). In Jungfrauoch,
NPF was limited to the availability of highly oxidized organic species, which was restricted by the contact time in the air



masses with the boundary layer (Bianchi et al., 2016). In Storm Peak Laboratory, NPF events were correlated with UV irradiance, but not with O₃ concentration and existing particle surface area (i.e. condensation sink) (Hallar et al., 2011). But at Chacaltaya Station in Bolivia, Maïdo observatory, and Jungfraujoch, the NPF frequency was found to be positively
60 correlated with CS, which was mainly because the increase of transmitted condensable precursors was often accompanied by the increase of CS (Rose et al., 2015; Rose et al., 2019; Boulon et al., 2010). These results indicated the location and seasonal effects of NPF at the high-altitude sites, and more measurements and studies were needed in high-altitude atmosphere.

The Tibetan Plateau (TP) is the largest plateau in China and the highest plateau in the world, with an average altitude
65 of over 4000 m a.s.l. It is known as the "roof of the world" and "the third pole" of the Earth and plays a fundamental role in the regional climate and environment through various dynamic and thermal effects (Yanai and Wu, 2006). Due to the rare anthropogenic activities, the TP is considered one of the most pristine locations around the world and an ideal location for characterizing remote and regional background aerosols. At the same time, NPF is an assumed key source of CCN production in the TP and has large impact on cloud processes, due to the negligible primary particle emissions. However,
70 research about NPF in the TP is rather limited. It restrained the understanding of mechanisms and CCN contribution of NPF in the TP, and brought considerable uncertainty about the radiative forcing. Some scientists have conducted the long-term NPF measurement at Himalayan Nepal Climate Observatory at Pyramid (NCO-P) site on the southern TP, and found that the NPF frequency varied in each season with the highest in the monsoon period (Venzac et al., 2008). The occurrence of NPF events in NCO-P was initiated by the up-valley winds which sent the biogenic condensable vapours from Khumbu
75 valley to the high-altitude location (Bianchi et al., 2021). At Mt. Yulong on the southeastern TP, the NPF frequency was only 14% during pre-monsoon season and the occurrence of NPF events was related to an elevated boundary layer or transported biomass burning pollutants from southern Asia, but not biogenic condensable vapours (Shang et al., 2018). Overall, few NPF studies were conducted in the central TP which can better represent the regional characteristics of TP compared with the southern and southeastern TP. The reason for the variation of NPF frequencies, the mechanisms for
80 nucleation and growth of nanoparticles, and CCN contribution of NPF in various seasons in the TP remained ambiguous.

In this study, intensive measurements were conducted at Nam Co station (4379 m a.s.l) in the central TP during pre-monsoon and monsoon seasons. Collocated measurements including particle number size distributions (PNSD), trace gases and meteorological parameters, and assisted Weather Research and Forecasting (WRF) and Community Multiscale Air Quality (CMAQ) models were employed to investigate the characteristics of PNSD and NPF. This study aimed to (1)
85 characterize NPF events in pre-monsoon and summer monsoon season in the central TP, (2) investigate the source of the



NPF events occurrence in pre-monsoon and summer monsoon season in the central TP, and (3) quantify the CCN contribution of NPF in pre-monsoon and summer monsoon season in the central TP.

2 Material and methods

2.1 Measurement site

90 An intensive field campaign was carried out at a high mountain observatory at the central Tibetan Plateau, i.e., Nam Co station (30.8°N, 91.0°E; 4730 m a.s.l) during the in-depth study of the atmospheric chemistry over the Tibetan Plateau in the year of 2019, referred as @Tibet 2019 field campaign (Fig. 1). The Nam Co station is located near Nam Co Lake (area: 1920 km²), the highest and largest saltwater lake in the world which is backed by the Nyainqentanglha mountains in the South. The ecology of the surrounding area is semi-arid land dominated by alpine meadow and barren areas. The capital city
95 (Lhasa) of the Tibet Autonomous Region is about 100 km southeast of the station. The closest town, Dangxiong, is about 70 km southeast of the station, between which are the Nyainqentanglha mountains. Overall, Nam Co station is located in a typical pristine environment and there are almost no local anthropogenic source emissions in this area. The measurement was conducted from 26 April to 22 May, 2019 and 15 June to 25 June, 2019, corresponding to the pre-monsoon season and the summer monsoon season, respectively (Bonasoni et al., 2010; Cong et al., 2015).

100 2.2 Instruments and methods

The sampling was conducted at the observatory field of Nam Co station (Fig. 1c). O₃ was detected using ultraviolet (UV) absorption by a “Model 49C Ozone Analyzer” (Thermo Scientific, USA). CO and water content (H₂O) were measured by Picarro G2401 based on cavity ring-down spectroscopy. Meteorological parameters including wind speed (WS), wind direction (WD), temperature (T) and relative humidity (RH) were measured by the automatic meteorological station (Met
105 one Instrument Inc). The photolysis frequencies of O₃ (JO¹D) were monitored using a spectral radiometer (ultra-fast CCD-detector spectrometer, METCON GmbH, Germany). 99 types of volatile organic compounds (VOC) were measured by an online gas chromatograph coupled with a mass spectrometer and flame ionization detectors (GC-MS/FID) (TH-PKU 300B, Wuhan Tianhong Instrument Co. Ltd., China) in pre-monsoon season (Wang et al., 2014). Black carbon (BC) was measured by Aethalometer (Magee Scientific, model AE33), and the concentration of BC at 880 nm was used in this study
110 to reduce the influence of Brown carbon (Kirchstetter et al., 2004).

PNSD in the stokes size range of 4nm and 700 nm were obtained by integrating two sets of scanning mobility particle spectrometers (SMPS). The first SMPS measured particles with the size of 4-45 nm, consisting of a TSI Model



3085 DMA and a TSI Model 3776 CPC (with a flow rate of 1.5 L min⁻¹). The second SMPS measured particles with the size of 45-700 nm, consisting of a TSI Model 3081 DMA and a TSI Model 3775 CPC (with a flow rate of 0.3 L min⁻¹). A silicon
 115 diffusion tube was placed before the SMPS, which kept the relative humidity (RH) of the sampling air under 40%. PNSD were corrected for particle losses in the SMPS and the sampling tube, following the method of “equivalent pipe length” as described in Wiedensohler et al. (2012).

Considering that the concentration of VOC in monsoon season has not been measured in this observation, Weather Research and Forecasting (WRF) (version 4.2.1) and The Community Multiscale Air Quality version 5.3.2 (CMAQv5.3.2)
 120 models have been adopted to simulate the VOC levels in the surrounding area to assist in the analysis of the role of VOC in NPF events. Similarly, SO₂ during pre-monsoon and monsoon was also simulated to help analyze the role of sulfuric acid in NPF events. Detailed information about the model setting and evaluation is provided in Text S1.

To reveal the transport pathway of air masses that arrive at the site, the 48h backward trajectories of the air mass at 600m above the ground (5330 m a.s.l) were computed using the HYSPLIT (Hybrid Single Particle Lagrangian Integrated
 125 Trajectory) model and Global Data Assimilation System (GDAS) data.

2.3 Parameterization of NPF

In this study, a typical NPF event was defined by the criteria that PN₃₋₁₀ (particle number concentration in the diameter of 3-10 nm) increased obviously, and lasted for more than 2 hours (Fang et al., 2020). The days without particle formation were defined as non-event days. Other days in which the increase of PN₃₋₁₀ was observed but lasted for less than 2 hours
 130 were treated as undefined days.

During the NPF events, the formation rate was calculated using the following formula (Cai and Jiang, 2017):

$$J_{d_k} = \frac{dN_{(d_k, d_u)}}{dt} + \sum_{d_g=d_k}^{d_u-1} \sum_{d_i=d_{min}}^{+\infty} \beta_{(i,g)} N_{(d_i, d_{i+1})} N_{(d_g, d_{g+1})} - \frac{1}{2} \sum_{d_g=d_{min}}^{d_u-1} \sum_{d_i^2=\max(d_{min}^2, d_k^2-d_{min}^2)}^{d_{i+1}^3+d_{g+1}^3 \leq d_u^3} \beta_{(i,g)} N_{(d_i, d_{i+1})} N_{(d_g, d_{g+1})} + n_u \cdot GR_u$$

(1)

135 Where J_{d_k} is the formation rate of particles at size d_k , and d_u is the upper size bound of the target size range. Here d_k and d_u are selected to be 4 and 25 nm, respectively. $N_{(d_k, d_u)}$ is the total number concentration of particles in the diameters of $[d_k, d_u]$. d_i is the lower bound of each measured size bin, and d_{min} is lowest size limit detected by measuring instrument. $\beta_{(i,g)}$ is the coagulation coefficient for the collision between the particle at size of d_i and the particle at size of d_g . n_u is the particle size distribution function (dN/dd_p). GR_u is the growth rate at size of d_u .



140 The growth rate (GR) was obtained by the mode-fitting method described in Dal Maso et al. (2005). In short, the PNSD during NPF event days were fitted as the sum of three-mode lognormal distribution. GR was calculated as the variation of the geometric mean diameter D_m of newly formed mode (4-25 nm) in unit interval (Dal Maso et al., 2005):

$$\text{GR} = \frac{\Delta D_m}{\Delta t}$$

(2)

145 To evaluate the scavenging effects of preexisting particles on condensable vapours, the condensation sink (CS) was calculated as follow (Dal Maso et al., 2005):

$$\text{CS} = 2\pi D \sum \beta_m(D_{p,i}) D_{p,i} N_i$$

(3)

where D is the diffusion coefficient of the condensing vapor, β_m is the transition regime correction factor, and $D_{p,i}$ and N_i are the diameter and number concentration in the size class i , respectively.

2.4 Calculation of CCN concentration

The CCN number concentration was calculated based on the assumption that particles larger than a certain diameter could act as CCN. The critical diameter (D_c) of the CCN activation at the supersaturation (S_c) can be calculated based on κ – Köhler theory (Petters and Kreidenweis, 2007):

155
$$\kappa = \frac{4A^3}{27D_c^3 \ln^2 S_c}$$

(4)

$$A = \frac{4\sigma_{s/a} M_w}{RT\rho_w}$$

(5)

Where κ is the hygroscopicity parameter about the composition-dependence of the solution water activity. $\sigma_{s/a}$ is the water surface tension (0.0728 N m⁻¹). M_w and ρ_w are the molecular weight and density of water, respectively. R is the universal gas constant (J mol⁻¹ K⁻¹), and T is the absolute temperature (K).

3 Results and discussions

3.1 Characteristics of meteorology and atmospheric pollutants

The distinct meteorological characterizations were exhibited in the two seasons. As shown in Fig. 2 and Fig. S4, 165 temperature behavior was characterized by higher value in monsoon season (10.4±4.1 °C) and lower value in pre-monsoon



season (3.1 ± 3.6 °C) with an average value of 5.3 ± 5.1 °C. The relative humidity (RH) seems very similar in the two seasons ($50\% \pm 21\%$ in pre-monsoon season vs $48\% \pm 19\%$ in monsoon season), but the water content (H_2O) in the air during monsoon season ($1.0\% \pm 0.2\%$) was clearly higher than that in pre-monsoon season ($0.6\% \pm 0.2\%$), which reflected the wetter environment in the monsoon period. Wind speed (WS) was comparable during the two seasons, which was 4.2 ± 2.7 m s⁻¹ in pre-monsoon season and 4.5 ± 2.7 m s⁻¹ in monsoon season, respectively. Wind direction (WD) showed a clear divergence, with westerly and southwesterly winds prevailing in pre-monsoon season, and southerly winds prevailing in monsoon season (Fig. S5). The frequencies of air masses arriving at the observation station from various directions during the two seasons were shown in Fig. S6. In pre-monsoon season, strong westerlies pass through western Nepal, northwest India and Pakistan (i.e., southern Himalayas). In monsoon season, air masses were derived from Bangladesh and northeast India and brought moisture that originated in the Bay of Bengal. The seasonality of meteorology was generally in agreement with the previous studies in the TP, which is strongly influenced by the large-scale Asian monsoon circulation (Cong et al., 2015; Bonasoni et al., 2010).

As a background high altitude site on the TP, the Nam Co station displayed a low particle concentration. On average $\text{PM}_{0.8}$ was 1.8 ± 1.0 $\mu\text{g m}^{-3}$, which was similar with PM_{10} (2 $\mu\text{g m}^{-3}$) measured by a high-resolution time-of-flight aerosol mass spectrometer at Nam Co station in 2015 (Xu et al., 2018a). The particulate matter concentration at Nam Co station was lower than the PM_{10} observed at Qomolangma Station (4.4 $\mu\text{g m}^{-3}$) on the southern TP and Waliguan Observatory (9.1 $\mu\text{g m}^{-3}$) on the northeastern TP, which resulted from a much longer transport distance of anthropogenic emissions compared with Qomolangma Station and Waliguan Observatory (Zhang et al., 2021). The average concentration of BC was 223 ± 135 ng m⁻³ during the whole measurement period, which was comparable with previous observations (Xu et al., 2018a; Xu et al., 2020; Wang et al., 2016; Xu et al., 2018b), and represented the background level in the TP region. The average O_3 concentration was 58 ± 15 ppbv, which was similar to the results from some high-elevation sites in the TP (Bonasoni et al., 2010; Shang et al., 2018) and higher than the results from Beijing during spring (Chen et al., 2020). Consistent with previous research (Xu et al., 2018a; Cong et al., 2015; Yin et al., 2021), higher PM, BC and O_3 concentrations were found during pre-monsoon season (Fig. S7). The higher BC and PM may result from the active biomass-burning emissions in pre-monsoon season on the southern TP (Cong et al., 2015). The higher O_3 in pre-monsoon season were primarily attributed to stratospheric intrusion of ozone (Yin et al., 2021). In contrast, there was no noticeable difference in CO between the two seasons, and the average concentration was 0.12 ± 0.14 ppmv.



3.2 Higher frequency of new particle formation in monsoon season

Fig. 2g shows the evolution of PNSD for the entire study. It can be seen that NPF events in the monsoon period were
195 observed almost every day (8 in 10 days, 80%), while the frequency of NPF events was extremely low during the
pre-monsoon period (4 in 27 days, 15%). As shown in Table 1, the event frequency at Nam Co station during monsoon
season was higher than the result reported at NCO-P site on the southern TP in monsoon season (57%) (Venzac et al., 2008),
and similar to the frequency reported at Mt. Daban on the northeastern TP in post-monsoon season (80%) (Du et al., 2015).
The frequency at Nam Co station during pre-monsoon season was lower than NCO-P (38%) (Venzac et al., 2008) and
200 comparable with Mt. Yulong on the southeastern TP (14%) (Shang et al., 2018) in the same season. In addition, the NPF
frequencies of other high-altitude sites, such as Mt. Tai (Lv et al., 2018), Jungfraujoch (Tröstl et al., 2016a), Maïdo
observatory (Rose et al., 2019), Storm Peak Laboratory (Hallar et al., 2011), were basically between those in pre-monsoon
and monsoon seasons of Nam Co station. In general, the frequencies of the two seasons at Nam Co station can represent the
highest and lowest values of NPF frequencies observed in the TP and other high-altitude sites, and even various
205 environments (such as urban, rural, etc.) (Nieminen et al., 2018).

Table 1 summarized the formation rate (J), growth rate (GR), and condensation sink (CS) at Nam Co station and other
high-altitude sites. The J at Nam Co station varied from 0.38 to 2.43 $\text{cm}^{-3} \text{s}^{-1}$, with an average value of $1.15 \pm 0.58 \text{ cm}^{-3} \text{ s}^{-1}$,
which was comparable with the results at Mt. Yulong (J_3 , 1.18 $\text{cm}^{-3} \text{ s}^{-1}$) (Shang et al., 2018) and Jungfraujoch ($J_{3,2}$, 0.2-7.5
 $\text{cm}^{-3} \text{ s}^{-1}$) (Tröstl et al., 2016a). However, the J at Nam Co station was higher than the values at NCO-P site (J_{10} , 0.14-0.19
210 $\text{cm}^{-3} \text{ s}^{-1}$) (Venzac et al., 2008) and Storm Peak Laboratory (J_8 , 0.39-1.19 $\text{cm}^{-3} \text{ s}^{-1}$) (Hallar et al., 2011), but lower than that at
Mt. Tai (J_3 , 1.33-52.54 $\text{cm}^{-3} \text{ s}^{-1}$) (Lv et al., 2018) and Maïdo observatory (J_2 , 0.5-30 $\text{cm}^{-3} \text{ s}^{-1}$) (Rose et al., 2019), which may
be due to the distinction of particle size range used in the calculation and precursor concentrations between the sites. For
example, SO_2 at Mt. Tai (3.2 ppb) (Lv et al., 2018) was much higher than that at Mt. Yulong (0.06 ppb) (Shang et al., 2018).
The average GR in the size range of 4-25 nm at Nam Co station varied from 1.5 to 5.6 nm h^{-1} , with the average value of 4.0
215 $\pm 1.2 \text{ nm h}^{-1}$, which was comparable with those at Mt. Yulong (3.2 nm h^{-1}) (Shang et al., 2018) and Jungfraujoch (4.0 nm h^{-1})
(Tröstl et al., 2016a), and higher than those at NCO-P site ($1.8 \pm 0.7 \text{ nm h}^{-1}$) (Venzac et al., 2008) and Mt. Daban (2.0
 nm h^{-1}) (Du et al., 2015), but lower than that at Maïdo observatory (8-45 nm h^{-1}) (Rose et al., 2019). The average CS was
 $0.15 \times 10^{-2} \pm 0.07 \times 10^{-2} \text{ s}^{-1}$ at Nam Co station, which was comparable with those at Mt. Yulong ($0.2 \times 10^{-2} \text{ s}^{-1}$) (Shang et al.,
2018), Maïdo observatory (0.02×10^{-2} - $2 \times 10^{-2} \text{ s}^{-1}$) (Rose et al., 2019) and Storm Peak Laboratory ($0.12 \times 10^{-2} \text{ s}^{-1}$) (Hallar et
220 al., 2011), and much lower than that at Mt. Tai (1.1×10^{-2} - $4.8 \times 10^{-2} \text{ s}^{-1}$) (Lv et al., 2018). In a word, the J , GR, and CS at
Nam Co station were within average levels in the high-altitude sites. Meanwhile, there was no significant variation in J , GR



and CS between pre-monsoon and monsoon seasons, although the NPF frequencies of the two seasons were quite different. The key factors determining the occurrence of NPF events need to be further studied.

3.3 Frequent NPF events driven by organic matter brought by summer monsoon

225 Whether an NPF event can occur was mainly related to 1) the CS, which mainly referred to the scavenging rate of precursors, clusters, and newly formed particles by background aerosols. High CS can lead to the continual reduction in newly formed particle number concentration, and inhibit the occurrence of NPF; 2) the gaseous precursors that can participate in nucleation and growth, including sulfuric acid (Kulmala et al., 2013), dimethylamine (Yao et al., 2018), ammonia (Xiao et al., 2015) and VOC (Tröstl et al., 2016b; Fang et al., 2020; Qiao et al., 2021). A sufficiently high
230 concentration of low volatility vapors (precursors) can contribute to persistent nucleation and generating new atmospheric particles; 3) meteorological factors including WD, RH, temperature, etc, which can influence the occurrence and intensity of NPF events by directly or indirectly affecting the source and sink parameters.

In the following, the discussion will focus on the key factors for the occurrence of NPF events described above. For clarity, NPF events days occurring in pre-monsoon and monsoon seasons were named NPF-pre days and NPF-monsoon
235 days, respectively. Non-events days in pre-monsoon season were termed non-event days, as non-event days in monsoon season were scarce.

3.3.1 Condensation sink

As shown in Fig. 3a, the levels of CS in NPF-pre days, NPF-monsoon days and non-event days were similar during 11:00–18:00 (the occurrence time of NPF events), although the CS in the early morning of NPF-pre days seems to be
240 slightly lower. The CS was mainly in the range of 0.1×10^{-2} – $0.15 \times 10^{-2} \text{ s}^{-1}$ during the NPF occurrence time, which was much lower than that at most locations in China, such as $\sim 0.01 \text{ s}^{-1}$ in urban Beijing (Deng et al., 2021), and 0.1×10^{-2} to $28.4 \times 10^{-2} \text{ s}^{-1}$ at Mt. Tai (Lv et al., 2018), and comparable with that at Mt. Yulong ($\sim 0.2 \times 10^{-2} \text{ s}^{-1}$) (Shang et al., 2018). The result varied from previous studies which reported much lower CS during NPF days than that in non-event days (Zhou et al., 2021; Lv et al., 2018). It indicated that the occurrence of NPF events at Nam Co station was not influenced by the lower CS.
245 The similar phenomenon was found at Mt. Yulong (Shang et al., 2018). In addition, previous studies found that CS was on average positively correlated with the occurrence of NPF events in some high-altitude observations at a larger scale, such as Maïdo observatory and Jungfraujoch (Rose et al., 2019; Boulon et al., 2010). When the gaseous precursors were transported to the observation site to trigger NPF events, the pre-existing particles were transported simultaneously and caused the



increase in CS. Although the topography and the rapidly changing conditions related to complex atmospheric dynamics at
250 Nam Co station were similar with Maïdo observatory and Jungfraujoch, the relationship between CS and the occurrence of
NPF events seemed different. Whatever, the result indicated that CS was not the decisive factor controlling the occurrence
of NPF events at Nam Co station.

3.3.2 Gas precursors

Gaseous sulfuric acid has been identified as the key precursor for nucleation and initial growth due to its low volatility
255 (Kulmala et al., 2013; Qiao et al., 2021), and the photochemical formation of SO₂ was the major source for sulfuric acid in
the atmosphere. However, the level of SO₂, the photochemical oxidation intensity of SO₂, and CS were comparable between
NPF days and non-event days, which indicated that sulfuric acid may not govern the occurrence of NPF events at Nam Co
station. Here, the low levels of SO₂ (0.03 ± 0.03 ppb) in NPF days and non-event days were present in Fig. S8. The
photochemical oxidation intensity of SO₂ was indicated by J (O¹D). As shown in Fig. 3b, NPF-pre days, NPF-monsoon
260 days and non-event days shared the same level of J (O¹D) ($3 \times 10^{-2} \cdot 6 \times 10^{-2} \text{ s}^{-1}$) during the occurrence time of NPF events.

In addition to sulfuric acid, organics were also considered to be an important factor of NPF events. Observations and
laboratory experiments have found that organics may participate in or even dominate the nucleation and growth process in
NPF events in pristine environments and the preindustrial atmosphere. For example, CLOUD (Cosmics Leaving Outdoor
Droplets) experiments observed obvious NPF events from highly oxidized organics without the involvement of sulfuric acid
265 (Kirkby et al., 2016). At the high-altitude sites of Jungfraujoch and Himalaya, NPF events occurred mainly through the
condensation of highly oxygenated molecules (HOMs) (Bianchi et al., 2016; Bianchi et al., 2021). Due to instrument status,
VOC measurement was only available in pre-monsoon season. The concentration of TVOC (total VOC) showed a
noticeably higher value (20%) during 11:00-18:00 on NPF-pre days compared with non-event days (Fig. 3c). Aromatics,
which can be used as the indicator of anthropogenic emissions, also exhibited a higher level (20%) during NPF-pre days
270 (Fig. 3d). This suggested that VOC may be the key factor in determining the occurrence of NPF events. In order to further
evaluate the role of VOC, we used WRF/CMAQ models to simulate the spatial distribution of VOC concentration in
pre-monsoon and monsoon seasons. It can be found that the average VOC concentration of NPF-monsoon days was about 2
ppb higher than that of NPF-pre days, and about 4 ppb higher than that of non-event days at Nam Co station (Fig. 4). In
addition, one recent research has found that the concentration of monoterpene-derived HOMs in East Asia was higher in
275 summer (June-August) than that in Spring (March-May) by using GEOS-Chem global chemical transport model (Xu et al.,
2022). All the results indicated that the frequent NPF events in monsoon season were caused by the higher concentration of



organic precursors. And pure organic nucleation may be the dominant NPF mechanism at Nam Co station.

3.3.3 Meteorology

While the concentrations of organic precursors have explained the notable distinction in NPF frequencies in
280 pre-monsoon season and monsoon season, the external factors driving the apparent difference in VOC levels between the
two seasons and other conditions that may affect the characteristics of NPF were still unknown. This indicated that a further
investigation into other NPF-related variables was still required.

WD can reflect the local situation for air mass and the source of air pollutants. The wind rose plots of non-event days,
NPF-pre days and NPF-monsoon days were present in Fig. 5. It can be found that the dominant WD on non-event days was
285 westerly and the WS was mostly below 10 m/s. In comparison, WD on NPF-pre days and NPF-monsoon days mainly come
from the South, mostly above 8 m/s. Similar patterns can be found from the time series (Fig. S2), that was, the WD from 3
May to 5 May (NPF-pre days) resembled that during summer monsoon, mainly from the South, and the overall WS was
relatively high. The example of the spatial distribution of wind in non-event days, NPF-pre days and NPF-monsoon days
showed the same phenomenon on a larger scale (Fig. S9). These results suggested that when the southerly wind with high
290 WD occurred, it may bring organic precursors from the southern region (northeast India) to Nam Co station, driving the
occurrence of NPF events in this area. This explained the phenomenon of the higher VOC concentration in NPF days than
non-event days. The frequent NPF events in monsoon season resulted from the higher concentration of organic vapours
brought by the frequent southerly wind (summer monsoon). This conclusion was confirmed by the more frequent air masses
from the South during monsoon season (Fig. S6). Similar result was found in the recent study which showed that the Indian
295 summer monsoon acted as a facilitator for transporting gaseous pollutants (Yin et al., 2021).

In Fig. 6, we showed the diurnal variations of meteorological factors during NPF-pre days, NPF-monsoon days and
non-event days at Nam Co station. First, the temperature in NPF-pre days and non-event days were generally close, but the
temperature of NPF-monsoon days was obviously higher. The similar temperature in NPF-pre days and non-event days
suggested that temperature was not a crucial factor for NPF event occurrence. Previous studies have found that higher
300 temperature can increase the formation rate of HOMs, but reduce the volatility of HOMs in the meanwhile. The effect of
temperature on the nucleation rate may not be important in a limited ambient temperature range (Stolzenburg et al., 2018).
But the higher temperature during NPF-monsoon days may promote monoterpene emissions, which favored particle
nucleation and growth (Andreae et al., 2022). This may explain the phenomenon for the higher VOC concentration in
NPF-pre days than NPF-monsoon days. Second, WS shared the same level during 11:00-18:00 on NPF days and non-event



305 days, while WS before the occurrence of NPF events in NPF days was higher than that of non-event days. Third, the average RH was similar in both NPF days and non-event days, although NPF-pre days had a wide range of RH changes. Laboratory studies have shown that water vapour can suppress the formation of extremely low volatility organic compounds (ELVOC) from monoterpenes (Bonn et al., 2002). However, our result was the opposite. During 11:00-18:00, the water content (H₂O) in the air during NPF-monsoon days was the highest, NPF-pre days was the second, and non-event days was
310 the lowest. This indicated the inhibition effect of water vapour was not important at Nam Co station. The similar finding was also observed at remote sites in the subboreal forest of North America (Andreae et al., 2022).

In all, the level of organic vapours governed the occurrence of NPF events at Nam Co station, while condensation sink and gaseous sulfuric acid had no effect. The frequent NPF events in summer monsoon season resulted from the higher concentration of organic vapours, which was brought from northeast India by the strong southerly monsoon.

315 3.4 Significant increase of CCN in monsoon season

The CCN concentration was estimated following the method introduced in Sect. 2.4. The hygroscopicity parameter κ was assumed to be a constant value of 0.12 throughout the measurement period, according to the previous measurement of chemical composition in TP (Shang et al., 2018). As a result, the D_c at S_c levels of 0.6% and 1.2% were 73.4 ± 1.3 and 46.3 ± 0.8 nm, respectively. No noticeable difference in D_c was found between pre-monsoon and monsoon seasons ($S_c =$
320 0.6%: 74.4 ± 1.0 vs 72.4 ± 1.1 nm, $S_c = 1.2\%$: 46.9 ± 0.6 vs 45.7 ± 0.7 nm). There could be uncertainties in the values of κ and D_c , but they had little impact on the final result of CCN concentration (Shang et al., 2018).

The aerosol production and CCN production during an NPF event can be obtained by comparing the particle number concentration at the beginning of the increase of the target particles (N_{init}) with the maximum number concentration (N_{max}), as introduced by Rose et al. (2017). The N_{init} and N_{max} are hourly average concentrations as shown in Fig. S10. Higher daily
325 aerosol production and CCN production were observed during monsoon season compared with that in pre-monsoon season (Fig.7). In monsoon season, Nucleation-mode particles (4-25 nm) started to increase quickly at around 11:00 when nucleation occurred. The freshly nucleated particles grew to larger sizes due to condensation and coagulation of the pre-existing particles within several hours, which contributed to the increase of Aitken-mode particles (25-100 nm) from 15:00. The average daily aerosol production of Nucleation-mode particles and Aitken-mode particles in monsoon season
330 was around 3400 cm^{-3} and 1200 cm^{-3} , respectively, and the enhancement factors (EFs, $N_{\text{max}}/N_{\text{init}}$) were 9.2 and 3.6, respectively. As for CCN, the average production of CCN at S_c of 0.6% and 1.2% in monsoon season was 180 and 518 cm^{-3} , respectively, and the EFs were 1.7 and 2.2, respectively. The EFs of CCN were lower than previous studies because



they only considered NPF days (Rose et al., 2017; Shen et al., 2016). Although the particles and CCN at around 11:00 in pre-monsoon season were comparable with monsoon season, the production of aerosols and CCN was much lower. The average daily aerosol production of Nucleation-mode particles and Aitken-mode particles in pre-monsoon season were around 500 cm⁻³ and 300 cm⁻³, respectively. And the CCN production at S_c of 0.6% and 1.2% was 170 and 286 cm⁻³, respectively. The average daily production of Nucleation-mode particles, Aitken-mode particles and CCN at S_c of 1.2% in monsoon season was 5.8, 3 and 0.8 times higher than that in pre-monsoon season, respectively.

The high-frequency NPF events in the summer monsoon period markedly increased the number concentration of atmospheric aerosols. The average PNSD during pre-monsoon and monsoon seasons were plotted in Fig. 8a with much higher number concentrations occurring during monsoon season. The mean total particle number concentration (PN₄₋₇₀₀) in monsoon season was 3647 ± 2671 cm⁻³, which was more than 2 times higher than that of pre-monsoon season (1163 ± 1026 cm⁻³). Although the measured particle size ranges were not the same with other studies, the results can still be comparable as the background particles were mainly distributed in tens to hundreds of nanometers. As shown in Table 1, PN₄₋₇₀₀ at Nam Co station in pre-monsoon season was comparable with other high-altitude sites around the world, while PN₄₋₇₀₀ in monsoon season was much higher due to the frequent NPF events. The atmospheric particles contributed by new particle nucleation and growth in monsoon season were mainly concentrated below 100 nm. Among them, the concentration of Nucleation-mode particles in monsoon season was about 2 times higher than that in pre-monsoon season, and the concentration of Aitken-mode particles was 3.5 times higher than that in pre-monsoon season. In contrast, Accumulation-mode particles (>100 nm) which were related to the secondary formation process and long-range transport (Wang et al., 2013; Vu et al., 2015), were nearly at the same level in the two seasons (around 200 cm⁻³). As shown in Fig. 9, the average number concentrations of CCN at S_c of 0.6% and 1.2% in monsoon season were 434 ± 242 and 863 ± 628 cm⁻³, respectively. The results were 10% and 56% higher than those in pre-monsoon season at S_c of 0.6% (396 ± 177 cm⁻³) and 1.2% (552 ± 261 cm⁻³).

It should be noted that the CCN concentration and production we estimated above were local ground levels, which can be considered as the minimum values. That is because those smaller particles (<40 nm) formed by NPF may further grow and reach CCN size in the following days during transportation, as the coagulation sink affecting the lifetime of aerosols was at a low level. This mechanism was verified at different high-altitude stations such as NCO-P site, Chacaltaya and Jungfraujoch (Venzac et al., 2008; Rose et al., 2015; Tröstl et al., 2016a). The Nucleation-mode and Aitken-mode particle bands in the morning reflected the continuation of NPF events. As a result, the amount of potential CCN in monsoon season could be much larger than the result measured here, due to the high level of the smaller particles. Therefore, the climate



effect from aerosols may have a large variance between pre-monsoon and monsoon season.

4 Summary and conclusions

The PNSD, trace gases and meteorological parameters were measured at Nam Co station (4379 m a.s.l) in the central Tibetan Plateau (TP) during pre-monsoon and summer monsoon seasons. Firstly, meteorological conditions between pre-monsoon and monsoon seasons were distinct with higher temperature and water content in monsoon season. Strong westerlies pass through western Nepal, northwest India and Pakistan in pre-monsoon season, while air masses were mainly derived from the South (Bangladesh and northeast India) in the monsoon period. Secondly, as the pristine high-altitude site, low levels of particles and gaseous pollutants were displayed at Nam Co station. Relatively higher pollutant concentration was found during pre-monsoon season due to less favorable atmospheric circulation.

The most important finding of this study was that there was an evident distinction in the frequencies of NPF events at Nam Co station with 15% in pre-monsoon season and 80% in monsoon season, which can represent the lowest and highest values of NPF frequencies observed in the TP and other high-altitude sites, even around the world. In addition, there was no noticeable variation in J , GR, and CS between pre-monsoon and monsoon seasons at Nam Co station. Through the comprehensive analysis of the measured CS, gaseous precursors and meteorological conditions, supplemented by the model simulations, we found that the level of organic vapours governed the occurrence of NPF events, while condensation sink and gaseous sulfuric acid had no effect. The frequent NPF events in monsoon season resulted from the higher concentration of organic vapours, which was brought from northeast India by the strong southerly monsoon.

The frequent NPF events in the summer monsoon season had elevated the number concentration of atmospheric aerosols and CCN at Nam Co station. The average daily production of Nucleation-mode particles, Aitken-mode particles and CCN at S_c of 1.2% in monsoon season was 5.8, 3 and 0.8 times higher than that in pre-monsoon season, respectively. The average total particle number concentration in monsoon season was more than 2 times higher than that in pre-monsoon season, mainly contributed by Nucleation-mode and Aitken-mode particles. And the average number concentration of CCN in monsoon season was 10%-56% higher than that in pre-monsoon season. Considering that the smaller particles (< 40 nm) formed by NPF may further grow and reach CCN size during the following days due to the low-level coagulation sink, the amount of potential CCN in monsoon season could be much larger than our local measurement results. It may markedly affect the earth's radiation balance and global climate. Our result emphasized the role of organic in the occurrence of NPF events in the TP. Seasonal effect of NPF should be considered in model simulations when calculating the amount of aerosols and CCN in high-altitude atmosphere.



390 *Data availability.* The data provided in this paper can be obtained from the author upon request (minhu@pku.edu.cn).

Supplement. An independent supplement document is available.

Authorship contributions. Lizi Tang: Investigation, Data curation, Methodology, Formal analysis, Writing - original draft,
395 Writing - review & editing. Min Hu: Project administration, Supervision, Funding acquisition, Writing - review & editing.
Dongjie Shang: Investigation, Data curation, Methodology, Formal analysis. Xin Fang: Investigation, Data curation,
Methodology, Formal analysis. Jianjiong Mao: Investigation, Data curation. Wanyun Xu: Data curation. Jiacheng Zhou:
Data curation. Weixiong Zhao: Data curation. Yaru Wang: Data curation. Chong Zhang: Data curation. Yingjie Zhang: Data
curation. Jianlin Hu: Data curation. Limin Zeng: Data curation. Chunxiang Ye: Project administration, Funding acquisition,
400 Data curation. Song Guo: Writing - review & editing. Zhijun Wu: Writing - review & editing.

Competing interests. The authors declare that they have no conflict of interest.

Acknowledgements. The research has been supported by the National Natural Science Foundation of China (91844301 and
405 91544214), National Research Program for Key Issues in Air Pollution Control (DQGG0103), National Key Research and
Development Program of China (No. 2016YFC0202000: Task 3), and the second Tibetan Plateau Scientific Expedition and
Research Program (STEP, 2019QZKK0601).

410

415



References

- Andreae, M. O., Andreae, T. W., Ditas, F., and Pöhlker, C.: Frequent new particle formation at remote sites in the subboreal forest of North America, *Atmos. Chem. Phys.*, 22, 2487-2505, 10.5194/acp-22-2487-2022, 2022.
- 420 Bianchi, F., Junninen, H., Bigi, A., Sinclair, V. A., Dada, L., Hoyle, C. R., Zha, Q., Yao, L., Ahonen, L. R., Bonasoni, P., Buenrostro Mazon, S., Hutterli, M., Laj, P., Lehtipalo, K., Kangasluoma, J., Kerminen, V. M., Kontkanen, J., Marinoni, A., Mirme, S., Molteni, U., Petäjä, T., Riva, M., Rose, C., Sellegri, K., Yan, C., Worsnop, D. R., Kulmala, M., Baltensperger, U., and Dommen, J.: Biogenic particles formed in the Himalaya as an important source of free tropospheric aerosols, *Nature Geoscience*, 14, 4-9, 10.1038/s41561-020-00661-5, 2021.
- 425 Bianchi, F., Tröstl, J., Junninen, H., Frege, C., Henne, S., Hoyle, C. R., Molteni, U., Herrmann, E., Adamov, A., Bukowiecki, N., Chen, X., Duplissy, J., Gysel, M., Hutterli, M., Kangasluoma, J., Kontkanen, J., Kürten, A., Manninen, H. E., Münch, S., Peräkylä, O., Petäjä, T., Rondo, L., Williamson, C., Weingartner, E., Curtius, J., Worsnop, D. R., Kulmala, M., Dommen, J., and Baltensperger, U.: New particle formation in the free troposphere: A question of chemistry and timing, *Science*, 352, 1109-1112, doi:10.1126/science.aad5456, 2016.
- 430 Bonasoni, P., Laj, P., Marinoni, A., Sprenger, M., Angelini, F., Arduini, J., Bonafè, U., Calzolari, F., Colombo, T., Decesari, S., Di Biagio, C., Di Sarra, A., Evangelisti, F., Duchi, R., Facchini, M. C., Fuzzi, S., Gobbi, G. P., Maione, M., Panday, A., Roccatò, F., Sellegri, K., Venzac, H., Verza, G., Villani, P., Vuillemoz, E., and Cristofanelli, P.: Atmospheric Brown Clouds in the Himalayas: first two years of continuous observations at the Nepal Climate Observatory-Pyramid (5079 m), *Atmospheric Chemistry and Physics*, 10, 7515-7531, 10.5194/acp-10-7515-2010, 2010.
- 435 Bonn, B., Schuster, G., and Moortgat, G. K.: Influence of Water Vapor on the Process of New Particle Formation during Monoterpene Ozonolysis, *The Journal of Physical Chemistry A*, 106, 2869-2881, 10.1021/jp012713p, 2002.
- Boulon, J., Sellegri, K., Venzac, H., Picard, D., Weingartner, E., Wehrle, G., Collaud Coen, M., Bütikofer, R., Flückiger, E., Baltensperger, U., and Laj, P.: New particle formation and ultrafine charged aerosol climatology at a high altitude site in the Alps (Jungfraujoch, 3580 m a.s.l., Switzerland), *Atmos. Chem. Phys.*, 10, 9333-9349, 10.5194/acp-10-9333-2010, 2010.
- 440 Cai, R. and Jiang, J.: A new balance formula to estimate new particle formation rate: reevaluating the effect of coagulation scavenging, *Atmos. Chem. Phys.*, 17, 12659-12675, 10.5194/acp-17-12659-2017, 2017.
- Chen, S., Wang, H., Lu, K., Zeng, L., Hu, M., and Zhang, Y.: The trend of surface ozone in Beijing from 2013 to 2019: Indications of the persisting strong atmospheric oxidation capacity, *Atmospheric Environment*, 242, 117801, <https://doi.org/10.1016/j.atmosenv.2020.117801>, 2020.
- 445 Cong, Z., Kang, S., Kawamura, K., Liu, B., Wan, X., Wang, Z., Gao, S., and Fu, P.: Carbonaceous aerosols on the south edge of the Tibetan Plateau: concentrations, seasonality and sources, *Atmos. Chem. Phys.*, 15, 1573-1584, 10.5194/acp-15-1573-2015, 2015.
- Dal Maso, M., Kulmala, M., Riipinen, I., and Wagner, R.: Formation and growth of fresh atmospheric aerosols: Eight years of aerosol size distribution data from SMEAR II, Hyytiälä, Finland, *Boreal Environment Research*, 10, 323-336, 2005.
- 450 Deng, C., Cai, R., Yan, C., Zheng, J., and Jiang, J.: Formation and growth of sub-3 nm particles in megacities: impact of background aerosols, *Faraday Discussions*, 226, 348-363, 10.1039/D0FD00083C, 2021.
- Du, W., Sun, Y. L., Xu, Y. S., Jiang, Q., Wang, Q. Q., Yang, W., Wang, F., Bai, Z. P., Zhao, X. D., and Yang, Y. C.: Chemical characterization of submicron aerosol and particle growth events at a national background site (3295 m a.s.l.) on the Tibetan Plateau, *Atmos. Chem. Phys.*, 15, 10811-10824, 10.5194/acp-15-10811-2015, 2015.
- 455 Fang, X., Hu, M., Shang, D., Tang, R., Shi, L., Olenius, T., Wang, Y., Wang, H., Zhang, Z., Chen, S., Yu, X., Zhu, W., Lou, S., Ma, Y., Li, X., Zeng, L., Wu, Z., Zheng, J., and Guo, S.: Observational Evidence for the Involvement of Dicarboxylic Acids in Particle Nucleation, *Environmental Science & Technology Letters*, 7, 388-394, 10.1021/acs.estlett.0c00270, 2020.
- Gordon, H., Kirkby, J., Baltensperger, U., Bianchi, F., Breitenlechner, M., Curtius, J., Dias, A., Dommen, J., Donahue, N.



- M., Dunne, E. M., Duplissy, J., Ehrhart, S., Flagan, R. C., Frege, C., Fuchs, C., Hansel, A., Hoyle, C. R., Kulmala, M.,
460 Kürten, A., Lehtipalo, K., Makhmutov, V., Molteni, U., Rissanen, M. P., Stozhkov, Y., Tröstl, J., Tsagkogeorgas, G., Wagner,
R., Williamson, C., Wimmer, D., Winkler, P. M., Yan, C., and Carslaw, K. S.: Causes and importance of new particle
formation in the present-day and preindustrial atmospheres, *Journal of Geophysical Research: Atmospheres*, 122,
8739-8760, <https://doi.org/10.1002/2017JD026844>, 2017.
- Hallar, A. G., Lowenthal, D. H., Chirokova, G., Borys, R. D., and Wiedinmyer, C.: Persistent daily new particle formation at
465 a mountain-top location, *Atmospheric Environment*, 45, 4111-4115, <https://doi.org/10.1016/j.atmosenv.2011.04.044>, 2011.
IPCC, 2021: *Climate Change 2021: The Physical Science Basis*. (eds [Masson-Delmotte, V. et al.] (Cambridge Univ. Press,
2021).
- Kerminen, V.-M., Chen, X., Vakkari, V., Petäjä, T., Kulmala, M., and Bianchi, F.: Atmospheric new particle formation and
growth: review of field observations, *Environmental Research Letters*, 13, 103003, [10.1088/1748-9326/aadf3c](https://doi.org/10.1088/1748-9326/aadf3c), 2018.
- 470 Kirchstetter, T. W., Novakov, T., and Hobbs, P. V.: Evidence that the spectral dependence of light absorption by aerosols is
affected by organic carbon, *Journal of Geophysical Research (Atmospheres)*, 109, D21208, [10.1029/2004jd004999](https://doi.org/10.1029/2004jd004999), 2004.
- Kirkby, J., Duplissy, J., Sengupta, K., Frege, C., Gordon, H., Williamson, C., Heinritzi, M., Simon, M., Yan, C., Almeida, J.,
Tröstl, J., Nieminen, T., Ortega, I. K., Wagner, R., Adamov, A., Amorim, A., Bernhammer, A.-K., Bianchi, F., Breitenlechner,
M., Brilke, S., Chen, X., Craven, J., Dias, A., Ehrhart, S., Flagan, R. C., Franchin, A., Fuchs, C., Guida, R., Hakala, J.,
475 Hoyle, C. R., Jokinen, T., Junninen, H., Kangasluoma, J., Kim, J., Krapf, M., Kürten, A., Laaksonen, A., Lehtipalo, K.,
Makhmutov, V., Mathot, S., Molteni, U., Onnela, A., Peräkylä, O., Piel, F., Petäjä, T., Praplan, A. P., Pringle, K., Rap, A.,
Richards, N. A. D., Riipinen, I., Rissanen, M. P., Rondo, L., Sarnela, N., Schobesberger, S., Scott, C. E., Seinfeld, J. H.,
Sipilä, M., Steiner, G., Stozhkov, Y., Stratmann, F., Tomé, A., Virtanen, A., Vogel, A. L., Wagner, A. C., Wagner, P. E.,
Weingartner, E., Wimmer, D., Winkler, P. M., Ye, P., Zhang, X., Hansel, A., Dommen, J., Donahue, N. M., Worsnop, D. R.,
480 Baltensperger, U., Kulmala, M., Carslaw, K. S., and Curtius, J.: Ion-induced nucleation of pure biogenic particles, *Nature*,
533, 521-526, [10.1038/nature17953](https://doi.org/10.1038/nature17953), 2016.
- Kulmala, M., Kontkanen, J., Junninen, H., Lehtipalo, K., Manninen, H., Nieminen, T., Petäjä, T., Sipilä, M., Schobesberger,
S., Rantala, P., Franchin, A., Jokinen, T., Järvinen, E., Äijälä, M., Kangasluoma, J., Hakala, J., Aalto, P., Paasonen, P.,
Mikkilä, J., and Worsnop, D.: Direct Observations of Atmospheric Aerosol Nucleation, *Science (New York, N.Y.)*, 339,
485 943-946, [10.1126/science.1227385](https://doi.org/10.1126/science.1227385), 2013.
- Lv, G., Sui, X., Chen, J., Jayaratne, R., and Mellouki, A.: Investigation of new particle formation at the summit of Mt. Tai,
China, *Atmos. Chem. Phys.*, 18, 2243-2258, [10.5194/acp-18-2243-2018](https://doi.org/10.5194/acp-18-2243-2018), 2018.
- Merikanto, J., Spracklen, D. V., Mann, G. W., Pickering, S. J., and Carslaw, K. S.: Impact of nucleation on global CCN,
Atmos. Chem. Phys., 9, 8601-8616, [10.5194/acp-9-8601-2009](https://doi.org/10.5194/acp-9-8601-2009), 2009.
- 490 Nieminen, T., Kerminen, V. M., Petäjä, T., Aalto, P. P., Arshinov, M., Asmi, E., Baltensperger, U., Beddows, D. C. S.,
Beukes, J. P., Collins, D., Ding, A., Harrison, R. M., Henzing, B., Hooda, R., Hu, M., Hörrak, U., Kivekäs, N., Komsaare,
K., Krejci, R., Kristensson, A., Laakso, L., Laaksonen, A., Leaitch, W. R., Lihavainen, H., Mihalopoulos, N., Németh, Z.,
Nie, W., O'Dowd, C., Salma, I., Sellegri, K., Svenningsson, B., Swietlicki, E., Tunved, P., Uleviccius, V., Vakkari, V., Vana,
M., Wiedensohler, A., Wu, Z., Virtanen, A., and Kulmala, M.: Global analysis of continental boundary layer new particle
495 formation based on long-term measurements, *Atmos. Chem. Phys.*, 18, 14737-14756, [10.5194/acp-18-14737-2018](https://doi.org/10.5194/acp-18-14737-2018), 2018.
- Peng, J. F., Hu, M., Wang, Z. B., Huang, X. F., Kumar, P., Wu, Z. J., Guo, S., Yue, D. L., Shang, D. J., Zheng, Z., and He, L.
Y.: Submicron aerosols at thirteen diversified sites in China: size distribution, new particle formation and corresponding
contribution to cloud condensation nuclei production, *Atmos. Chem. Phys.*, 14, 10249-10265, [10.5194/acp-14-10249-2014](https://doi.org/10.5194/acp-14-10249-2014),
2014.
- 500 Petters, M. D. and Kreidenweis, S. M.: A single parameter representation of hygroscopic growth and cloud condensation
nucleus activity, *Atmos. Chem. Phys.*, 7, 1961-1971, [10.5194/acp-7-1961-2007](https://doi.org/10.5194/acp-7-1961-2007), 2007.



- Qiao, X., Yan, C., Li, X., Guo, Y., Yin, R., Deng, C., Li, C., Nie, W., Wang, M., Cai, R., Huang, D., Wang, Z., Yao, L., Worsnop, D. R., Bianchi, F., Liu, Y., Donahue, N. M., Kulmala, M., and Jiang, J.: Contribution of Atmospheric Oxygenated Organic Compounds to Particle Growth in an Urban Environment, *Environmental Science & Technology*, 55, 13646-13656, 10.1021/acs.est.1c02095, 2021.
- 505
- Rose, C., Foucart, B., Picard, D., Colomb, A., Metzger, J. M., Tulet, P., and Sellegri, K.: New particle formation in the volcanic eruption plume of the Piton de la Fournaise: specific features from a long-term dataset, *Atmos. Chem. Phys.*, 19, 13243-13265, 10.5194/acp-19-13243-2019, 2019.
- Rose, C., Sellegri, K., Moreno, I., Velarde, F., Ramonet, M., Weinhold, K., Krejci, R., Andrade, M., Wiedensohler, A., Ginot, P., and Laj, P.: CCN production by new particle formation in the free troposphere, *Atmos. Chem. Phys.*, 17, 1529-1541, 10.5194/acp-17-1529-2017, 2017.
- 510
- Rose, C., Sellegri, K., Velarde, F., Moreno, I., Ramonet, M., Weinhold, K., Krejci, R., Ginot, P., Andrade, M., Wiedensohler, A., and Laj, P.: Frequent nucleation events at the high altitude station of Chacaltaya (5240 m a.s.l.), Bolivia, *Atmospheric Environment*, 102, 18-29, <https://doi.org/10.1016/j.atmosenv.2014.11.015>, 2015.
- 515
- Shang, D., Hu, M., Zheng, J., Qin, Y., Du, Z., Li, M., Fang, J., Peng, J., Wu, Y., Lu, S., and Guo, S.: Particle number size distribution and new particle formation under the influence of biomass burning at a high altitude background site at Mt. Yulong (3410 m), China, *Atmos. Chem. Phys.*, 18, 15687-15703, 10.5194/acp-18-15687-2018, 2018.
- Shen, X., Sun, J., Zhang, X., Zhang, Y., Zhang, L., and Fan, R.: Key features of new particle formation events at background sites in China and their influence on cloud condensation nuclei, *Frontiers of Environmental Science & Engineering*, 10, 5, 10.1007/s11783-016-0833-2, 2016.
- 520
- Stolzenburg, D., Fischer, L., Vogel, A. L., Heinritzi, M., Schervish, M., Simon, M., Wagner, A. C., Dada, L., Ahonen, L. R., Amorim, A., Baccarini, A., Bauer, P. S., Baumgartner, B., Bergen, A., Bianchi, F., Breitenlechner, M., Brilke, S., Buenrostro Mazon, S., Chen, D., Dias, A., Draper, D. C., Duplissy, J., El Haddad, I., Finkenzeller, H., Frege, C., Fuchs, C., Garmash, O., Gordon, H., He, X., Helm, J., Hofbauer, V., Hoyle, C. R., Kim, C., Kirkby, J., Kontkanen, J., Kürten, A., Lampilahti, J., Lawler, M., Lehtipalo, K., Leiminger, M., Mai, H., Mathot, S., Mentler, B., Molteni, U., Nie, W., Nieminen, T., Nowak, J. B., Ojdanic, A., Onnela, A., Passananti, M., Petäjä, T., Quéléver, L. L. J., Rissanen, M. P., Sarnela, N., Schallhart, S., Tauber, C., Tomé, A., Wagner, R., Wang, M., Weitz, L., Wimmer, D., Xiao, M., Yan, C., Ye, P., Zha, Q., Baltensperger, U., Curtius, J., Dommen, J., Flagan, R. C., Kulmala, M., Smith, J. N., Worsnop, D. R., Hansel, A., Donahue, N. M., and Winkler, P. M.: Rapid growth of organic aerosol nanoparticles over a wide tropospheric temperature range, *Proceedings of the National Academy of Sciences of the United States of America*, 115, 9122-9127, 10.1073/pnas.1807604115, 2018.
- 530
- Tröstl, J., Herrmann, E., Frege, C., Bianchi, F., Molteni, U., Bukowiecki, N., Hoyle, C. R., Steinbacher, M., Weingartner, E., Dommen, J., Gysel, M., and Baltensperger, U.: Contribution of new particle formation to the total aerosol concentration at the high-altitude site Jungfrauoch (3580 m asl, Switzerland), *Journal of Geophysical Research: Atmospheres*, 121, 11,692-611,711, <https://doi.org/10.1002/2015JD024637>, 2016a.
- 535
- Tröstl, J., Chuang, W. K., Gordon, H., Heinritzi, M., Yan, C., Molteni, U., Ahlm, L., Frege, C., Bianchi, F., Wagner, R., Simon, M., Lehtipalo, K., Williamson, C., Craven, J. S., Duplissy, J., Adamov, A., Almeida, J., Bernhammer, A.-K., Breitenlechner, M., Brilke, S., Dias, A., Ehrhart, S., Flagan, R. C., Franchin, A., Fuchs, C., Guida, R., Gysel, M., Hansel, A., Hoyle, C. R., Jokinen, T., Junninen, H., Kangasluoma, J., Keskinen, H., Kim, J., Krapf, M., Kürten, A., Laaksonen, A., Lawler, M., Leiminger, M., Mathot, S., Möhler, O., Nieminen, T., Onnela, A., Petäjä, T., Piel, F. M., Miettinen, P., Rissanen, M. P., Rondo, L., Sarnela, N., Schobesberger, S., Sengupta, K., Sipilä, M., Smith, J. N., Steiner, G., Tomé, A., Virtanen, A., Wagner, A. C., Weingartner, E., Wimmer, D., Winkler, P. M., Ye, P., Carslaw, K. S., Curtius, J., Dommen, J., Kirkby, J., Kulmala, M., Riipinen, I., Worsnop, D. R., Donahue, N. M., and Baltensperger, U.: The role of low-volatility organic compounds in initial particle growth in the atmosphere, *Nature*, 533, 527-531, 10.1038/nature18271, 2016b.
- 540
- Venzac, H., Sellegri, K., Laj, P., Villani, P., Bonasoni, P., Marinoni, A., Cristofanelli, P., Calzolari, F., Fuzzi, S., Decesari, S.,



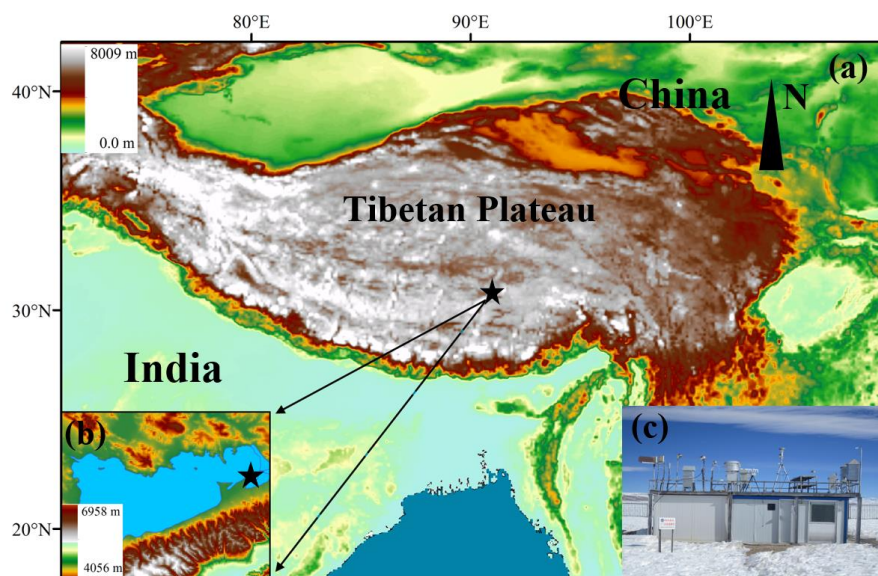
- 545 Facchini, M.-C., Vuillemoz, E., and Verza, G. P.: High frequency new particle formation in the Himalayas, *Proceedings of the National Academy of Sciences*, 105, 15666-15671, doi:10.1073/pnas.0801355105, 2008.
Vu, T. V., Delgado-Saborit, J. M., and Harrison, R. M.: Review: Particle number size distributions from seven major sources and implications for source apportionment studies, *Atmospheric Environment*, 122, 114-132, <https://doi.org/10.1016/j.atmosenv.2015.09.027>, 2015.
- 550 Wang, M., Xu, B., Wang, N., Cao, J., Tie, X., Wang, H., Zhu, C., and Yang, W.: Two distinct patterns of seasonal variation of airborne black carbon over Tibetan Plateau, *Science of The Total Environment*, 573, 1041-1052, <https://doi.org/10.1016/j.scitotenv.2016.08.184>, 2016.
Wang, M., Zeng, L., Lu, S., Shao, M., Liu, X., Yu, X., Chen, W., Yuan, B., Zhang, Q., Hu, M., and Zhang, Z.: Development and validation of a cryogen-free automatic gas chromatograph system (GC-MS/FID) for online measurements of volatile organic compounds, *Analytical Methods*, 6, 9424-9434, 10.1039/C4AY01855A, 2014.
- 555 Wang, Z., Wu, Z., Yue, D., Shang, D., Guo, S., Sun, J., Ding, A., Wang, L., Jiang, J., Guo, H., Gao, J., Cheung, H. C., Morawska, L., Keywood, M., and Hu, M.: New particle formation in China: Current knowledge and further directions, *Science of The Total Environment*, 577, 258-266, <https://doi.org/10.1016/j.scitotenv.2016.10.177>, 2017.
Wang, Z. B., Hu, M., Wu, Z. J., Yue, D. L., He, L. Y., Huang, X. F., Liu, X. G., and Wiedensohler, A.: Long-term measurements of particle number size distributions and the relationships with air mass history and source apportionment in the summer of Beijing, *Atmos. Chem. Phys.*, 13, 10159-10170, 10.5194/acp-13-10159-2013, 2013.
- 560 Wiedensohler, A., Birmili, W., Nowak, A., Sonntag, A., Weinhold, K., Merkel, M., Wehner, B., Tuch, T., Pfeifer, S., Fiebig, M., Fjåraa, A. M., Asmi, E., Sellegri, K., Depuy, R., Venzac, H., Villani, P., Laj, P., Aalto, P., Ogren, J. A., Swietlicki, E., Williams, P., Roldin, P., Quincey, P., Hüglin, C., Fierz-Schmidhauser, R., Gysel, M., Weingartner, E., Riccobono, F., Santos, S., Gröning, C., Faloon, K., Beddows, D., Harrison, R., Monahan, C., Jennings, S. G., O'Dowd, C. D., Marinoni, A., Horn, H. G., Keck, L., Jiang, J., Scheckman, J., McMurry, P. H., Deng, Z., Zhao, C. S., Moerman, M., Henzing, B., de Leeuw, G., Löschau, G., and Bastian, S.: Mobility particle size spectrometers: harmonization of technical standards and data structure to facilitate high quality long-term observations of atmospheric particle number size distributions, *Atmos. Meas. Tech.*, 5, 657-685, 10.5194/amt-5-657-2012, 2012.
- 570 Xiao, S., Wang, M. Y., Yao, L., Kulmala, M., Zhou, B., Yang, X., Chen, J. M., Wang, D. F., Fu, Q. Y., Worsnop, D. R., and Wang, L.: Strong atmospheric new particle formation in winter in urban Shanghai, China, *Atmos. Chem. Phys.*, 15, 1769-1781, 10.5194/acp-15-1769-2015, 2015.
Xu, J., Hettiyadura, A. P. S., Liu, Y., Zhang, X., Kang, S., and Laskin, A.: Regional Differences of Chemical Composition and Optical Properties of Aerosols in the Tibetan Plateau, *Journal of Geophysical Research: Atmospheres*, 125, e2019JD031226, <https://doi.org/10.1029/2019JD031226>, 2020.
- 575 Xu, J., Zhang, Q., Shi, J., Ge, X., Xie, C., Wang, J., Kang, S., Zhang, R., and Wang, Y.: Chemical characteristics of submicron particles at the central Tibetan Plateau: insights from aerosol mass spectrometry, *Atmos. Chem. Phys.*, 18, 427-443, 10.5194/acp-18-427-2018, 2018a.
Xu, R., Tie, X., Li, G., Zhao, S., Cao, J., Feng, T., and Long, X.: Effect of biomass burning on black carbon (BC) in South Asia and Tibetan Plateau: The analysis of WRF-Chem modeling, *Science of The Total Environment*, 645, 901-912, <https://doi.org/10.1016/j.scitotenv.2018.07.165>, 2018b.
- 580 Xu, R., Thornton, J. A., Lee, B. H., Zhang, Y., Jaeglé, L., Lopez-Hilfiker, F. D., Rantala, P., and Petäjä, T.: Global simulations of monoterpene-derived peroxy radical fates and the distributions of highly oxygenated organic molecules (HOMs) and accretion products, *Atmos. Chem. Phys.*, 22, 5477-5494, 10.5194/acp-22-5477-2022, 2022.
- 585 Yanai, M. and Wu, G.-X.: Effects of the Tibetan Plateau, in: *The Asian Monsoon*, edited by: Wang, B., Springer Berlin Heidelberg, Berlin, Heidelberg, 513-549, 10.1007/3-540-37722-0_13, 2006.
Yao, L., Garmash, O., Bianchi, F., Zheng, J., Yan, C., Kontkanen, J., Junninen, H., Mazon, S., Ehn, M., Paasonen, P., Sipilä,



- M., Wang, M., Wang, X., Xiao, S., Chen, H., Lu, Y., Zhang, B., Wang, D., Fu, Q., and Wang, L.: Atmospheric new particle formation from sulfuric acid and amines in a Chinese megacity, *Science*, 361, 278-281, 10.1126/science.aao4839, 2018.
- 590 Yin, X., Kang, S., Zhang, Q., and Zang, G.: Study of air pollutants in the inland Tibetan Plateau (Nam Co Station), *Chinese Journal of Nature*, 42(5), 373-378, 10.3969/j.issn.0253-9608.2020.05.003, 2020.
- Yin, X., Kang, S., Foy, B. d., Rupakheti, D., Rupakheti, M., Cong, Z., Wan, X., Zhang, G., and Zhang, Q.: Impacts of Indian summer monsoon and stratospheric intrusion on air pollutants in the inland Tibetan Plateau, *Geoscience Frontiers*, 12, 101255, <https://doi.org/10.1016/j.gsf.2021.101255>, 2021.
- 595 Zhang, X., Xu, J., Kang, S., Sun, J., Shi, J., Gong, C., Sun, X., Du, H., Ge, X., and Zhang, Q.: Regional Differences in the Light Absorption Properties of Fine Particulate Matter Over the Tibetan Plateau: Insights From HR-ToF-AMS and Aethalometer Measurements, *Journal of Geophysical Research: Atmospheres*, 126, e2021JD035562, <https://doi.org/10.1029/2021JD035562>, 2021.
- 600 Zhou, Y., Hakala, S., Yan, C., Gao, Y., Yao, X., Chu, B., Chan, T., Kangasluoma, J., Gani, S., Kontkanen, J., Paasonen, P., Liu, Y., Petäjä, T., Kulmala, M., and Dada, L.: Measurement report: New particle formation characteristics at an urban and a mountain station in northern China, *Atmos. Chem. Phys.*, 21, 17885-17906, 10.5194/acp-21-17885-2021, 2021.

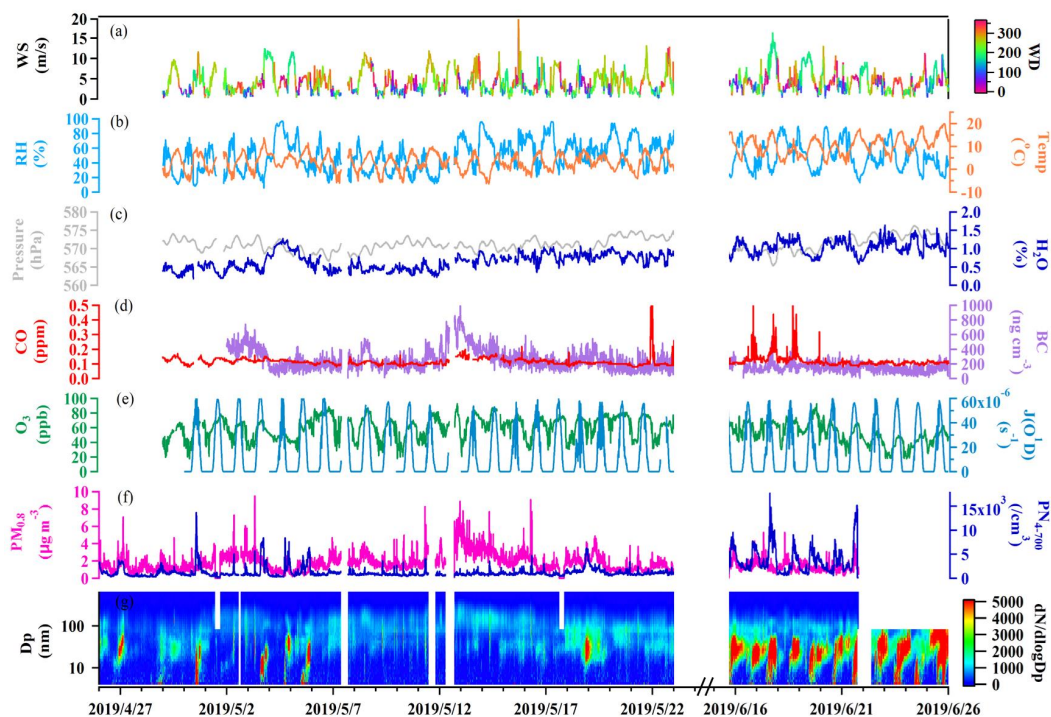
605

610



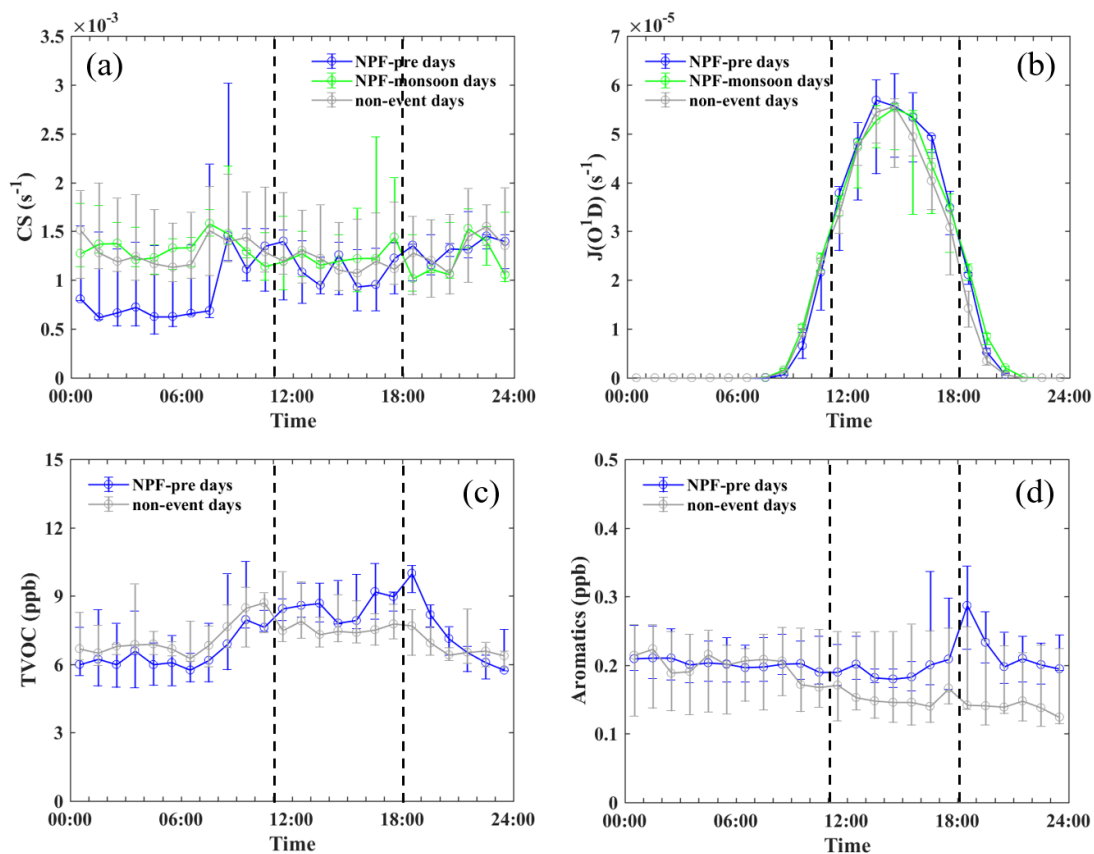
615 **Figure 1.** Location map for (a) the Tibetan Plateau, (b) Nam Co station, colored according to altitude. (c) The appearance
drawing of atmospheric environment observatory field of Nam Co station (Yin et al., 2020).

620



625 **Figure 2.** Time series during pre-monsoon and monsoon: (a) the wind speed and wind direction, (b) the ambient
temperature and the relative humidity (RH), (c) the pressure and water content (H₂O) in air, (d) CO concentration and the
black carbon (BC) concentration, (e) O₃ concentration and the photolysis frequencies of O₃ (JO¹D), (f) the PM_{0.8} mass
concentration and the number concentration of particles in size of 4-700 nm (PN₄₋₇₀₀), (g) the particle number size
distribution (PNSD).

630



635

Figure 3. Diurnal variations of (a) condensation sink (CS), (b) JO^1D , the total concentration of (c) VOC (TVOC) and (d) aromatics in NPF-pre days, NPF-monsoon days and non-event days.

640

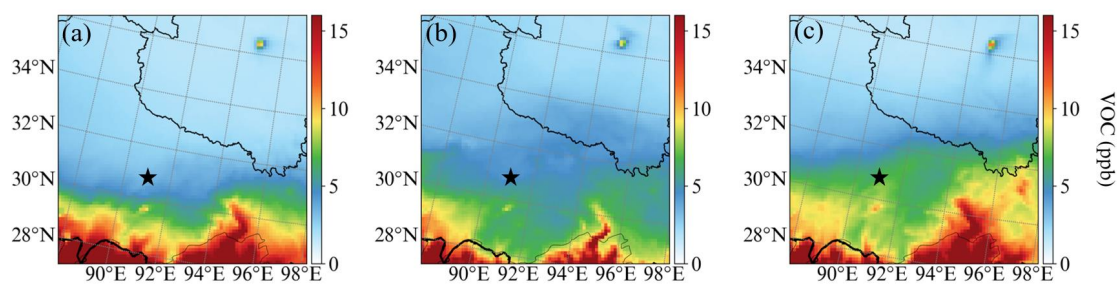


Figure 4. Model spatial distribution of TVOC during (a) non-event days, (b) NPF-pre days, and (c) NPF-monsoon days.

645 The star is Nam Co station.

650

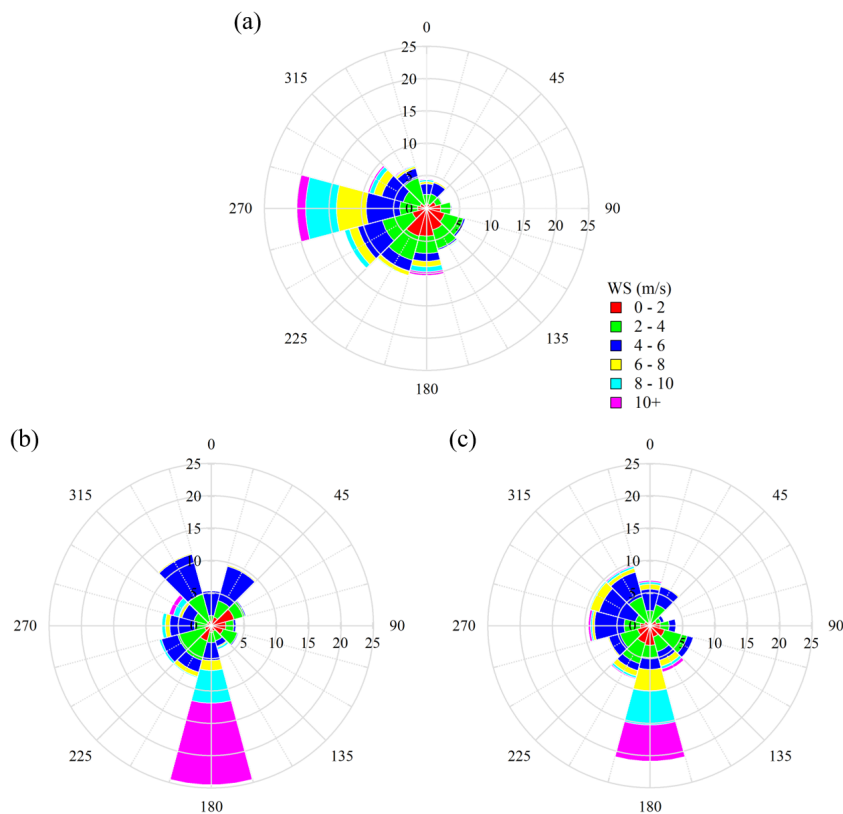


Figure 5. Wind rose plots of (a) non-event days, (b) NPF-pre days and (c) NPF-monsoon days. The length of each spoke on the circle represents the probability of wind coming from a particular direction at a certain range of wind speed.

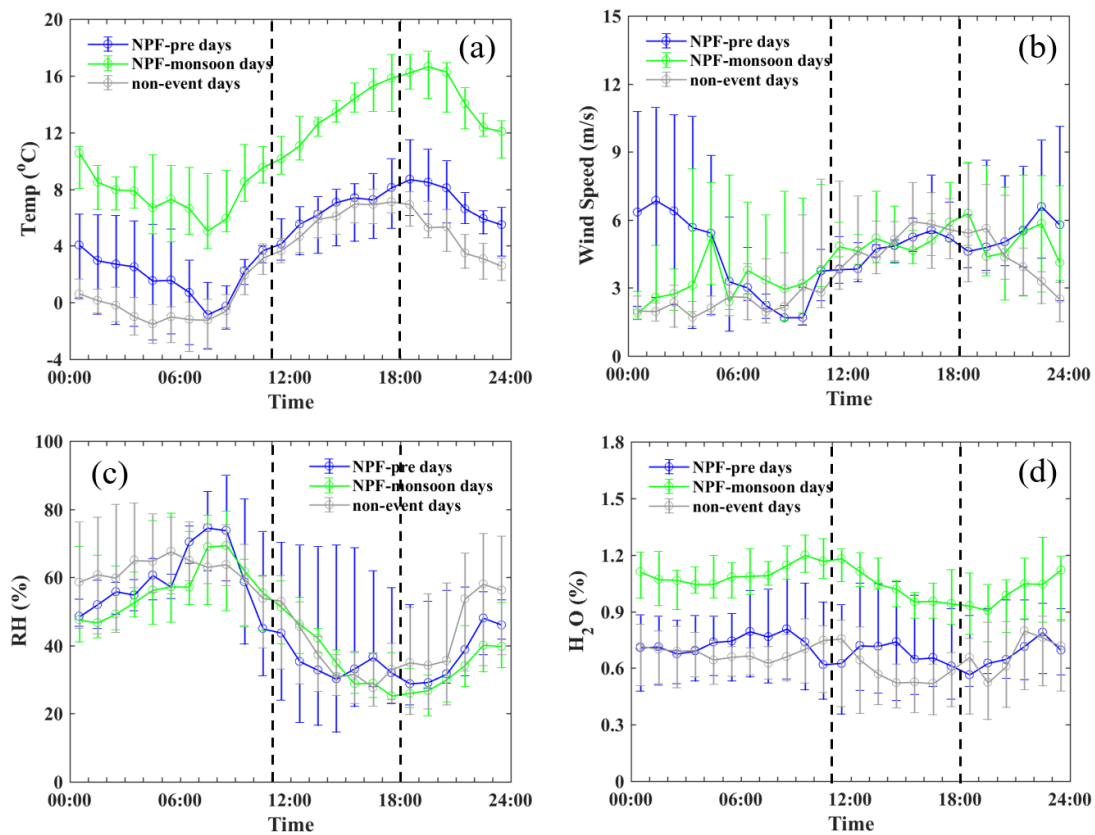


Figure 6. Diurnal variations of (a) temperature, (b) wind speed, (c) RH and (d) the water content (H₂O) in the air in NPF-pre days, NPF-monsoon days and non-event days.

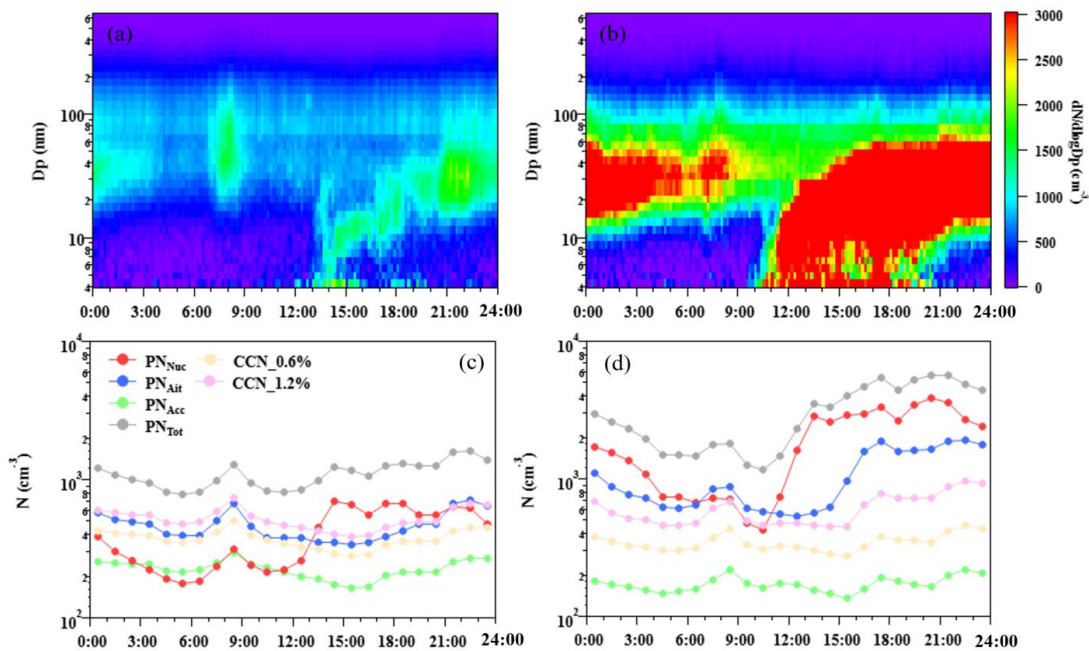
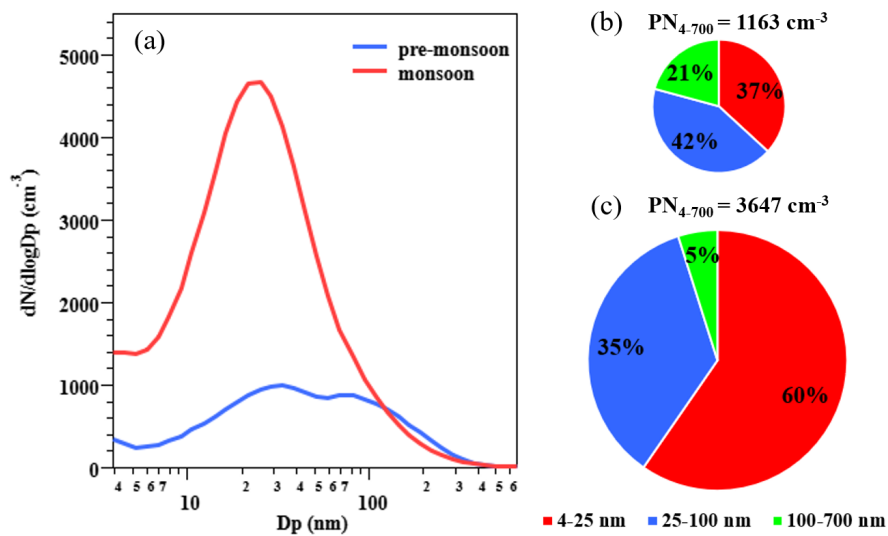


Figure 7. Diurnal variations of particle number size distributions (PNSD) and the number concentrations of Nucleation-mode particles (PN_{Nuc}), Aitken-mode particles (PN_{Ait}), Accumulation-mode particles (PN_{Acc}), the total particles (PN_{Tot}), CCN at S_c of 0.6% ($\text{CCN}_{0.6\%}$) and 1.2% ($\text{CCN}_{1.2\%}$) during pre-monsoon (a and c) and monsoon (b and d) seasons.



670

Figure 8. Particle number size distribution (PNSD) at Nam Co station. (a) Mean PNSD in pre-monsoon and monsoon; the contribution of different size ranges (4-25 nm, 25-100 nm, 100-700 nm) to the total particle number concentration (b) in pre-monsoon and (c) in monsoon.

675

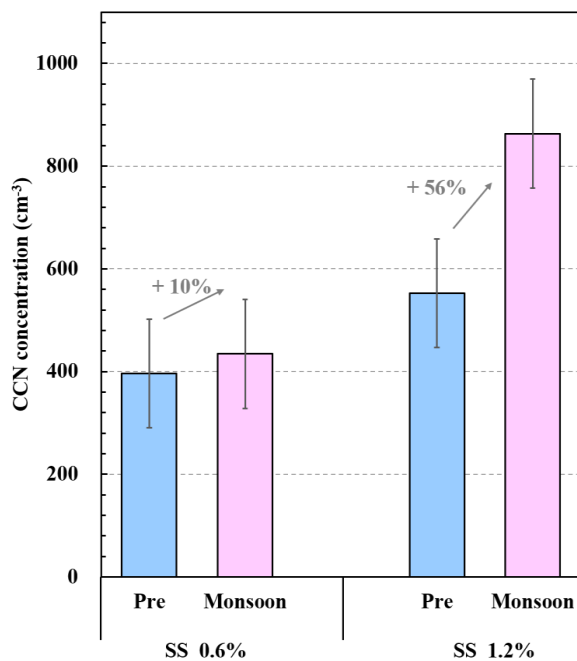


Figure 9. Mean number concentration of CCN at S_c of 0.6% and 1.2% in pre-monsoon and monsoon seasons.

680

685

690



Table 1. Comparison of particle number concentration (PN) and NPF parameters (NPF frequency, CS, J, GR) with other high-altitude sites around the world

Site	Altitude (m)	Observation Date and season ^a	PN (cm ⁻³)	NPF frequency	CS×10 ⁻² (s ⁻¹)	J ^b (cm ⁻³ s ⁻¹)	GR ^c (nm h ⁻¹)	Reference
Nam Co station, China	4379	May 2019, pre-monsoon	1163±1026 (PN ₃₋₇₀₀)	15%	0.14±0.07	1.11±0.79 (J _i)	4.2±0.9 (GR ₄₋₂₅)	This study
		June 2019 monsoon	3647±2671 (PN ₃₋₇₀₀)	80%	0.15±0.05	1.08±0.21 (J _i)	3.8±0.8 (GR ₄₋₂₅)	
NCO-P ^d , Nepal	5079	April-June 2007, pre-monsoon	NA	38%	NA	0.14 (J ₁₀)	1.8±0.7	Venzac et al. (2008)
		July-September 2007, monsoon	NA	57%	NA	0.19 (J ₁₀)	NA	
Mt. Daban, China	3295	September-October 2013, post-monsoon	2400 (PN ₁₂₋₄₇₈)	80%	NA	NA	2.0	Du et al. (2015)
Mt. Yulong, China	3410	May-April 2015, pre-monsoon	1600±1290 (PN ₃₋₁₀₀₀₀)	14%	0.2	1.18 (J ₃)	3.2	Shang et al. (2018)
Mt. Tai, China	1534	July-August 2014, summer	NA	21%	1.1-4.8	1.33-52.54 (J ₃)	1.15-7.76 (GR ₃₋₂₀)	Lv et al. (2018)
Jungfrauoch, Switzerland	3580	July 2013-June 2014, one year	200-1000 (PN ₁₀₋₆₀₀)	20%	NA	0.2-7.5 (J _{3,2})	4±2.3 (GR ₅₋₁₅)	Tröstl et al. (2016a)
Maido observator, Réunion	2165	2015, one year	NA	67%	0.02-2	0.5-30 (J ₂)	8-45 (GR ₁₂₋₁₉)	Rose et al. (2019)
Storm Peak Laboratory, USA	3210	March-May 2001-2009, spring	NA	56%	0.12±0.05	0.39±0.05 (J ₆)	7.5±4.5	Hallar et al. (2011)
		June-July 2001-2009, summer	NA	43%	0.13±0.06	1.19±0.34 (J ₈)	9.1±6.9	

695 ^a The seasons in Tibet measurements were divided into pre-monsoon, monsoon and post-monsoon seasons. The seasons not in Tibet measurements were divided into spring, summer, autumn and winter.

^b The subscript indicated the *J* of particles at the certain size.

^c The subscript indicated the particle size range used for calculation of GR. No explanation meant that it was not specified in the literatures.

700 ^d Nepal Climate Observatory at Pyramid site



NA: Data not found in the literatures